Available online at www.sciencedirect.com
SCIENCE DIRECT®
Journal of the European Ceramic Society 25 (2005) 663–672
www.elsevier.com/locate/jeurceramsoc

The role of the synthesis route to obtain densified TiO_2-doped alumina ceramics

T. Hernandez*, M. C. Bautista

CIEMAT, Avenida Complutense 22, 28040 Madrid, Spain

Received 8 June 2003; received in revised form 20 January 2004; accepted 25 January 2004

Available online 10 June 2004

Abstract

Alumina specimens doped with 1 wt.% of titanium oxide were successfully prepared by three different synthesis routes: Pechini method, coprecipitation and sol–gel processes. This paper describes the phase sequence in each synthesis process and its effect on the final particle size and shape, as well as, on the microstructure of the calcined powders and the sintering behaviour. The intermediate phases to obtain α-alumina were κ-Al_2O_3, θ-Al_2O_3 and γ-$Al_2O_3$for the Pechini, coprecipitation and sol–gel processes, respectively, as could be detected by FT-IR and XRD. Secondly, the calcined powders were isopressed and sintered at 1625 °C for 4 h. Density measurements, and microstructure were investigated by Archimedes method and TEM/SEM, respectively. The sintering behaviour of the materials is discussed on the basis of the characteristic of the metastable phases obtained by each route. Coprecipitation yielded rounded particles with the smallest size. Sol–gel process produced larger grains with vermicular shapes and Pechini method led to hexagonal corundum crystals.

Keywords: Al_2O_3; Sol–gel processes; Coprecipitation; Pechini method; Al_2O_3–TiO_2

1. Introduction

The titania-doped alumina ceramics can be used in many applications. Membranes with controlled porosity obtained by the sol–gel synthesis[1,2] can be used from gas separation to biomedical processes. The alumina–titania mixed oxides were reported to have both acidic and basic sites at the surface, and therefore, this material can be used as support for transition metal catalyst.[3] TiO_2-doped alumina is also interesting because of its electronic[4] and optical applications.[5] On the other hand, it is well known that the addition of a small amount of certain additives, such as TiO_2, to α-Al_2O_3, considerably changes its sintering behaviour to manufacture dense materials.[6] The typical bimodal sintered microstructure of the monolithic material contained α-alumina platelets in an equiaxed matrix is dramatically changed when different dopants are added, showing a mixed microstructure composed by anisotropic grains embedded in the original equiaxial matrix. Extensive literature describes the grain growth during sintering as well as the tendency of alumina to develop anisotropic tabular grains[7] and segregations at grain boundaries.[8] The phase transitions of monolithic aluminas with the temperature have also been studied previously.[9] However, there are not many published works about the influence of the synthesis method on the polymorphic transitions of doped alumina and on the microstructure of the final ceramic obtained after sintering at high temperatures.

It is well-known that the powder sinterability and the mechanical properties of sintered materials depend on the purity and the particle characteristics of the starting powder. The wet chemical methods for ceramic synthesis are capable of yielding reactive powders that sinter at relative low temperatures, producing non-agglomerated fine particles with narrow particle size distribution.

In the present work, three of the most well-known wet processes[10] are compared: Pechini method, controlled precipitation and sol–gel processes. The effect of the synthesis process on the particle size, morphology and sintering behaviour of 1 wt.% titania-doped alumina is discussed.

* Corresponding author. Tel.: +34-91-346-6770; fax: +34-91-346-6005.
E-mail address: tesa@ciemat.es (T. Hernandez).

0955-2219/$ – see front matter © 2004 Elsevier Ltd. All rights reserved.
doi:10.1016/j.jeurceramsoc.2004.01.013

2. Experimental procedures

2.1. Sample preparation

The three routes showed in Fig. 1 have been used to prepare titanium-doped alumina with a titanium content of 1 wt.%. The three methods were labelled as "P/Ti" for Pechini process, "C/Ti" for coprecipitation, and "S/Ti" for the sol–gel route.

The Pechini method[11] leads to polybasic quelates formed between the α-hydroxycarboxylic (lactic acid 85%, Aldrich) and metallic ions coming from aluminium nitrate nona-hydrate (Merck extra pure) and titanium nitrate(IV). Previously, titanium(IV) isopropoxide (97%, Aldrich) was mixed with 65% nitric acid in order to obtain the former titanium nitrate. The pH of the final solution was about 2. The chelate underwent polyesterification on heating at 90 °C and stirring with a polyfunctional alcohol. Further heating (175 °C) produced a viscous resin that is transformed to a rigid transparent glassy gel. The dehydrated gel at that temperature was attrition milled during four hours and 60 μm sieved. Finally the precursor oxide was obtained by heating from this at 450 °C.

Multicomponent oxides can be prepared by coprecipitation through intermediate precipitates.[12] Extrapure non-ahydrate aluminium nitrate (Merck) and titanium(IV) isopropoxide 97% (Aldrich) were used as starting materials at pH ∼9 in this process. The precipitate was washing to pH ∼7 and stirred by using an IKA ultra-turrax T 50 to prevent the agglomerates. An intimate mixture of components was formed during precipitation. The precipitate was dried at 60 °C and afterwards, 60 μm sieved. This process allows maintaining the chemical homogeneity at high temperature calcination.

For the sol–gel processing of metal–organic compounds, titanium(IV) isopropoxide 97% (Aldrich) and aluminium tri-*sec*-butoxide (Alfa Chemical Co.) were mixed in alcohol media to achieve the required ceramic composition.[13] Acid hydrolysis was carried out under controlled additions of water and nitric acid at room temperature to obtain an ultra-fine precipitate. A highly dispersed stable colloidal solution was obtained by peptisation at 80 °C during 48 h and finally a gel was obtained. Such gel was dried at 60 °C and milled in an agatha mortar.

Different calcination temperatures were used as a function of the thermal behaviour observed for each sample from the thermal analysis data. The calcinated samples were isopressed at 200 MPa and sintered in air at 1625 °C for four hours.

2.2. Characterisation methods

The crystalline phases as a function of temperature were analysed by X-ray diffraction (XRD, Philips diffractometer X-Pert-MPD) with Cu Kα radiation and Si monochomator. Termogravimetry (TG) and differential thermal analysis (DTA) tests were done ranging from room temperature to 1200 °C at 10 °C/min, using a SEIKO TG/DTA 6300 equipment, to evaluate the phase transformation temperatures of the titania-doped alumina. Intermediate species from the precursors to the final α-alumina were detected by infrared spectroscopy (IR) employing a NICOLET, Magna IR spectometer in the range of 4000–400 cm^{-1}. The calcinated powders were studied by transmission electron microscopy

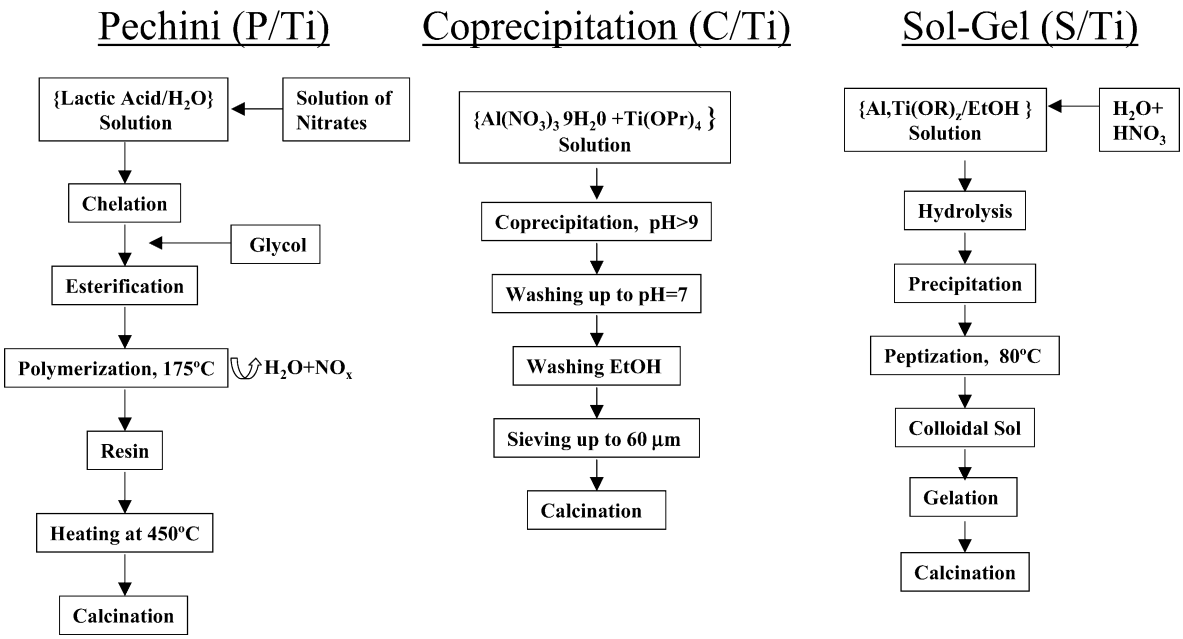

Fig. 1. Flow diagrams for the three procedures used for powder synthesis.

TEM-EDX (Philips CM200FEG at 200 kV and 2.35 Å of structural resolution). A scanning electron microscope (SEM, JEOL JSM 6400 at 20 kV and ADX LINK INCA) was used to study the microstructure of mirror-like polished and thermally etched sintered samples. The average grain size was estimated by the interception method of at least 100 grains from SEM micrographs.

3. Results

3.1. TG/DTA analysis

Fig. 2 shows the TG/DTA measurements for the same composition (1 wt.% titania-doped alumina) prepared by the three routes depicted above. Fig. 2a, corresponding to the Pechini process, shows a great and progressive weight loss (75.2%) up to ∼700 °C. In this range of temperature three exothermic peaks (280, 390 and 550 °C) characteristic of the Pechini synthesis are clearly defined which correspond to a charring sequence with different stable semi-decomposed species.[14] From 700 to 1200 °C the weight loss is ∼3% and the two small peaks detected at 870 and 1200 °C in the DTA can be associated to the formation of κ- and α-alumina phases, respectively, as it will be demonstrated later.

Thermal analysis differs greatly in the coprecipitation route (Fig. 2b). In this case a narrow and sharp endothermic peak was found around 260 °C which is associated with a large weight loss on TG curve (38.1%). This peak is related to a very early decomposition of gibbsite ($Al(OH)_3$) into γ-alumina, as will be seen later by FT-IR and XRD. From 600 to 1200 °C the weight loss is about 2.4% and the single peak detected at 1000 °C indicates the crystallisation of θ-alumina. Complementary information about this process will be presented in the XRD section.

The thermal behaviour of the powder from the sol–gel route is shown in Fig. 2c where three endothermic low temperatures peaks can be observed. The first one at about 50 °C can be associated to the alcohol elimination. The endothermic peak at 100 °C corresponds to the removal of physically adsorbed water molecules from the pores of boehmite. A third endothermic effect is observed at 200 °C with an overlapped shoulder at 260 °C. In this range of temperatures, the sample continuously loses water molecules, most probably due to dehydration and loss of OH^-. At intermediate temperatures from 260 to 450 °C, the organic matter is burned and the DTA curve shows an exothermic band typical of a continuous reaction without well-defined thermal events which is characteristic of an amorphous structure. The weight loss during the process up to 600 °C is 75%.

Crystallisation of γ-Al_2O_3 is indicated by the exothermic DTA peak at 850 °C, while the corundum phase appears at about 1100 °C, as will be seen in the XRD section. The weight loss from 600 to 1200 °C was 1.5%.

3.2. XRD analysis

Fig. 3 shows X-ray diffractograms of the powder samples obtained by the three synthesis methods and treated at different temperatures, allowing to compare the phase evolution with temperature. In the case of the Pechini route, the first phase transition observed by the thermal analysis corresponded to κ-Al_2O_3. In effect, the powder was amorphous up to 800 °C been conformed to a charred resin in which the aluminium–oxygen bonds were randomised. Above this temperature, a metastable intermediate major phase was identified as κ-Al_2O_3, although an incipient corundum signal was also present. The κ-alumina phase signal decreased as temperature raised in contrast with the corundum peaks that constantly enhanced. Only a well-crystallised corundum phase was found at 1125 °C (Fig. 3a).

During the coprecipitation process, a poor crystalline phase, compatible with γ-Al_2O_3, was formed around 300 °C (Fig. 3b), probably as consequence of the gibbsite decomposition. Calcination up to 925 °C did not produce any changes in the crystalline phase, and only around 1125 °C the θ-Al_2O_3 phase was formed.

The sol–gel process produced a transition sequence to α-alumina different than the other two alumina synthesis processes (Fig. 3c). The first crystallisation occurs at about 850 °C to γ-Al_2O_3 and this phase transformed to full α-alumina by heating at 1125 °C.

3.3. IR spectra

Fig. 4 shows the FT-IR spectra of P/Ti (Fig. 4a), C/Ti (Fig. 4b) and S/Ti (Fig. 4c) samples with different thermal treatments. The 4000–1000 cm^{-1} spectral region shows the absorption bands of the O–H stretching (3700–3200 cm^{-1}), O–H bending (1650–1200 cm^{-1}) and other organic bonds vibration modes. The absorption bands at the wavelengths from 1000 to 400 cm^{-1} are mainly due to the Al–O vibrational modes. For the three synthesis routes used to obtain titania-doped alumina, the effect of the temperature on the infrared spectra is clearly observed.

The Pechini synthesis as well as the change of the organic species implicated in the organic compounds pyrolysis up to 450 °C has been widely explained in a previous paper.[12] The absorption band at 1740 cm^{-1} was assigned to the stretching vibration mode of the carbonyl group in the ester compound because of the reaction of the lactic acid and ethylene glycol in the Pechini procedure (Fig. 4a). The bands of the organic compounds sharply decrease as the temperature increases being a consequence of the organic material thermal decomposition. The absorption band at 3227 cm^{-1} also diminishes due to the water molecules loss. At 850 °C a sharp and well-defined band at 442 cm^{-1} was assigned to the corundum phase. The overlapped bands at 750, 650 and 571 cm^{-1} indicate a disordered phase of the aluminium oxide. This phase has been identified as κ-alumina through XRD pattern. At 1125 °C a better resolved spectrum has

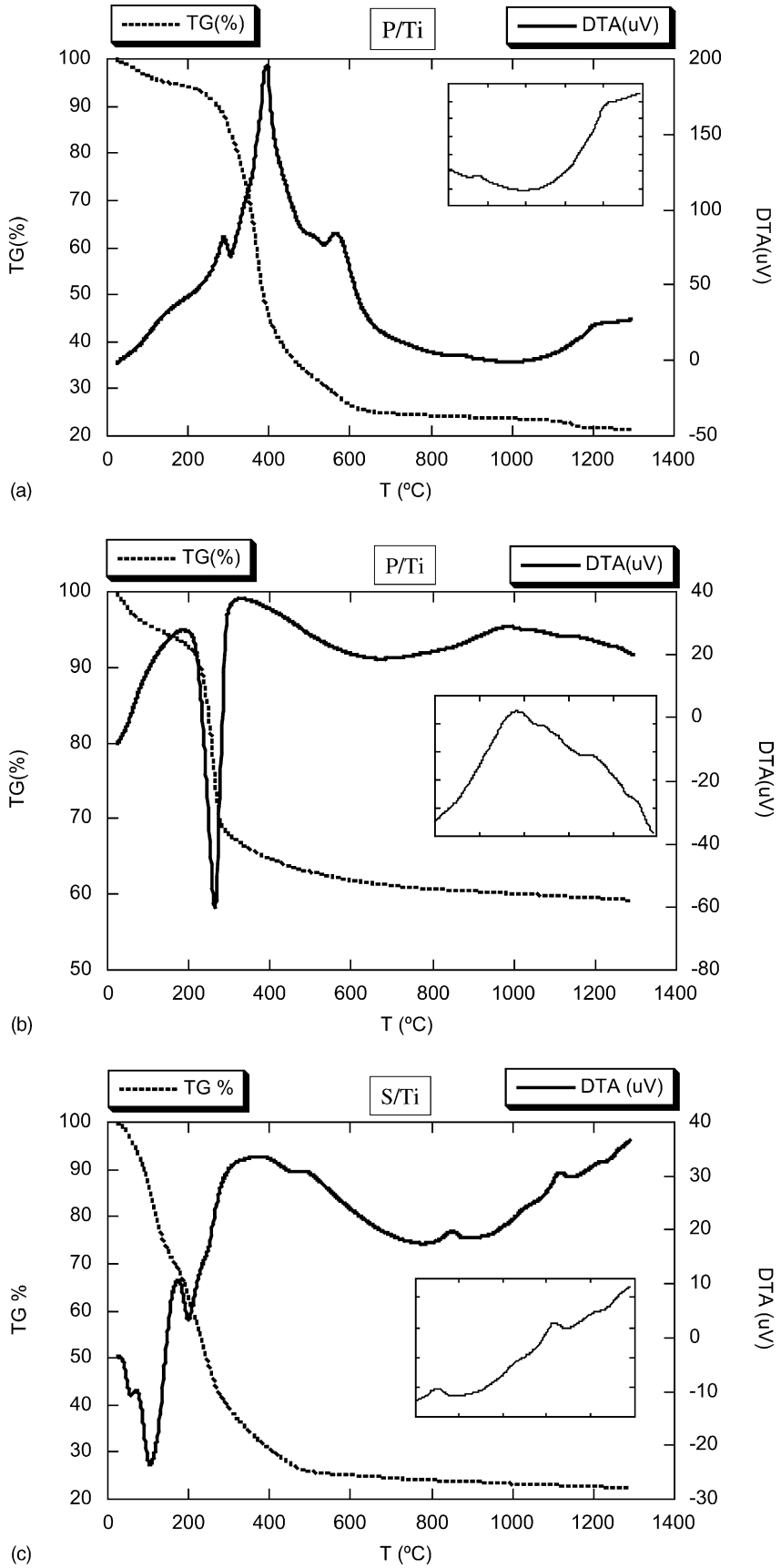

Fig. 2. TG/DTA analyses for the 1 wt.% titania-doped alumina prepared by: (a) Pechini process, (b) coprecipitation and (c) sol–gel.

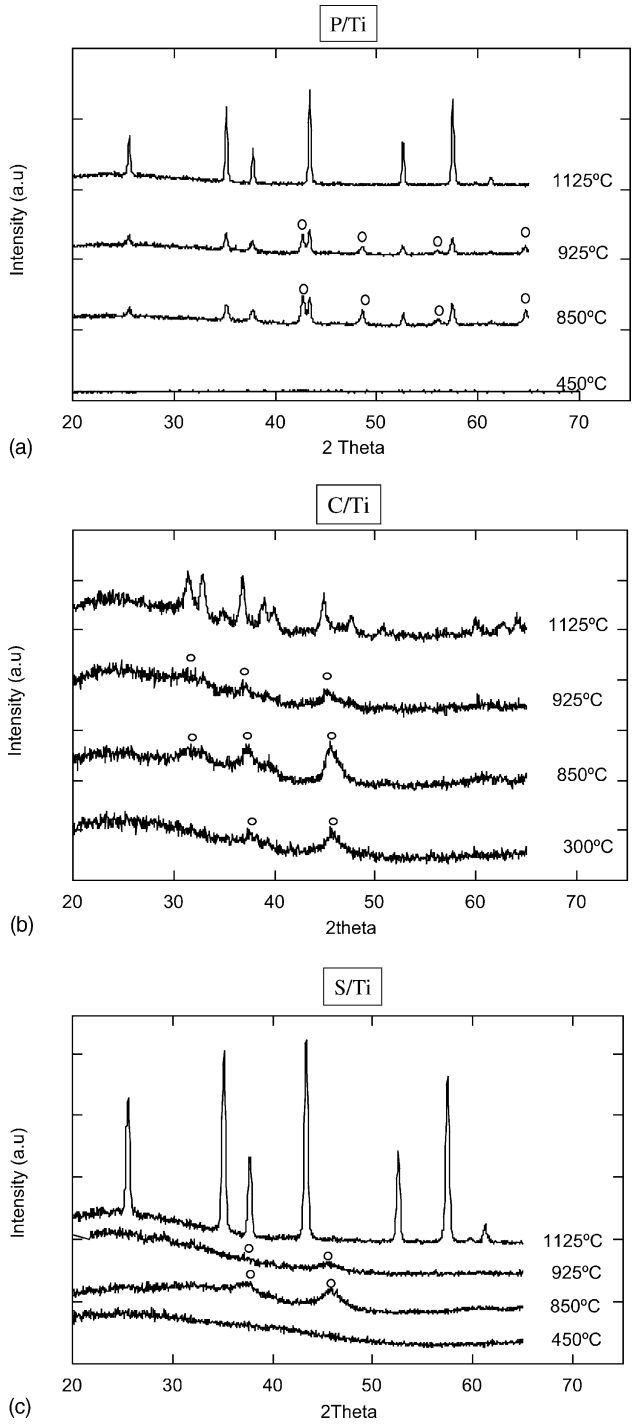

Fig. 3. Phase evolution with temperature in the powders following the synthesis procedure: (a) Pechini (open circles are κ-Al_2O_3, unmarked peaks α-Al_2O_3), (b) coprecipitation (open circles are γ-Al_2O_3, unmarked peaks θ-Al_2O_3) and (c) sol–gel (open circles γ-Al_2O_3, unmarked peaks α-Al_2O_3).

been obtained and the sharply bands at 447 and 490 cm^{-1} confirmed the fine structure of α-alumina, although remainders of the unstable κ-phase can be observed.

The C/Ti sample infrared spectra (Fig. 4b) shows a different evolution with respect to the Pechini process. The absorption bands around 3000 cm^{-1} due to the stretching motions of the O–H species stay up to 950 °C, which confirms the presence of gibbsite (Al–O–OH). Rama Rao et al.[15] reported stretching modes of Al–O–H at 3300 cm^{-1} with a smoothed shoulder at 3090 cm^{-1} and bending modes at 1070 and 1160 cm^{-1}. Given that a wide infrared band between 1000 and 1300 cm^{-1} is observed in the spectrum at 25 °C, it does not allow us distinguish the former bending mode absorption bands. The stretching motion of the O–H in free water also appears in this region and is confirmed by the bending mode absorption band at 1630 cm^{-1}. It is not feasible to attain any information about the Al–O vibration modes in this spectrum because the spectrum is not resolved below 950 cm^{-1}.

At 300 °C the water content clearly diminishes and the IR spectrum in the range of 500–1000 cm^{-1} shows a broad and smooth absorption band, which can be attributed to the disordered distribution of vacancies and the continuous distribution of bonds length in an amorphous material. At higher calcinations temperature, 950 °C, the IR spectrum resolved showing a double peak.[16] A small peak centred at about 690 cm^{-1} can be associated to a small percentage of θ-alumina in the sample. This third peak is perfectly defined at 1125 °C, as well as those found at the 450, 550 and 830 cm^{-1}. All of them confirm that the phase detected at this temperature is θ-Al_2O_3.

The sample obtained by sol–gel (S/Ti, Fig. 4c) presents an evolution from an amorphous phase to the corundum phase (α-Al_2O_3) through γ-Al_2O_3. At low temperatures (room temperature and 450 °C) the infrared spectra bands in the range 400–1000 cm^{-1} are characteristic of amorphous species. At 850 °C there is not any important change, the organic material has been almost removed and the spectral region with a high profusion of bands between 400 and 1000 cm^{-1} is better resolved. At 925 °C, two broad bands centred at 757 and 565 cm^{-1} can be observed, indicating the formation of γ-Al_2O_3, which is in accordance to the X-ray diffractograms. Finally, at 1125 °C, a phase transition takes place from γ-Al_2O_3, to a highly ordered structure of α-Al_2O_3, as it can be confirmed by its characteristic absorption bands at 653, 571 and 441 cm^{-1}. The results described in this section are in accordance with the X-ray diffraction data.

3.4. Powder morphology and microstructure

Fig. 5 shows the TEM photographs of the powders obtained after the thermal treatment at 1125 °C for the three methods studied. Shape and size of the powders differ significantly depending on the followed route. P/Ti particles (Fig. 5a) have hexagonal morphology corresponding to corundum single crystals with about 1 μm in diameter. There is a low degree of particle agglomeration as a consequence of the previous resin processing.

The particles obtained by the coprecipitation method (C/Ti), Fig. 5b, present a noticeable smaller size (down to

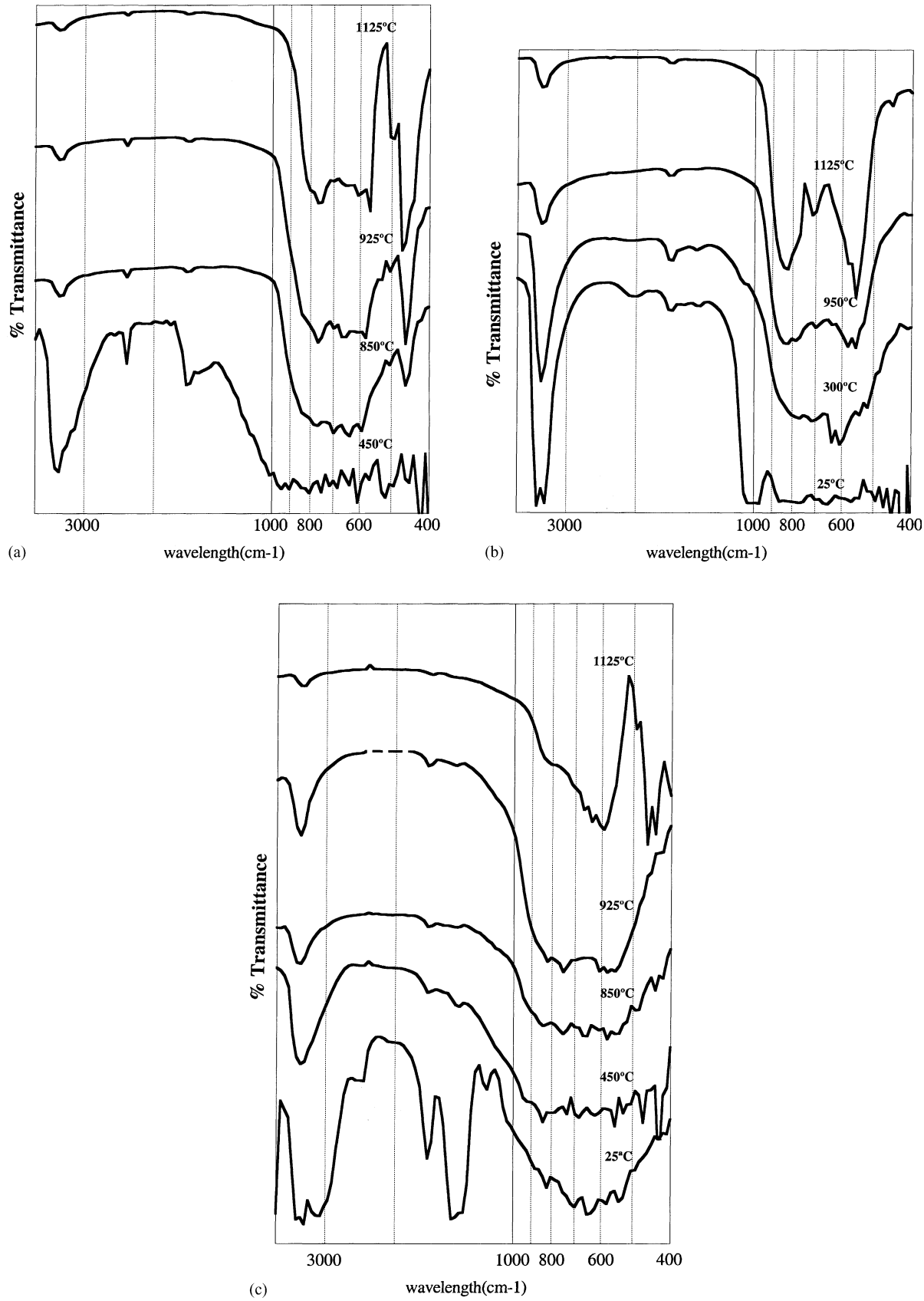

Fig. 4. Optical transmittance spectra in the infrared region vs. calcination temperature of 1 wt.% titania-doped alumina synthesised by: (a) P/Ti sample, (b) C/Ti sample and (c) S/Ti sample.

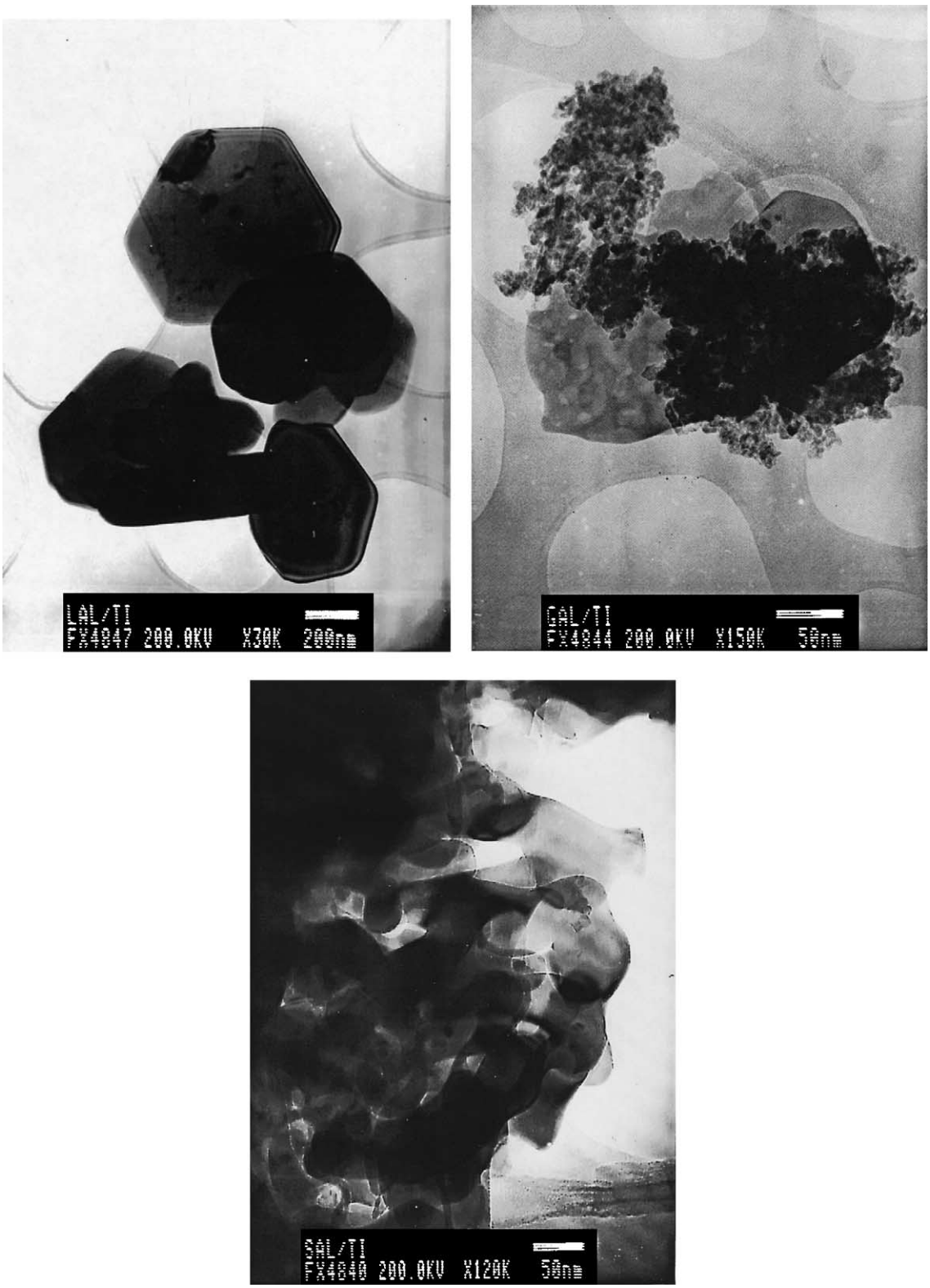

Fig. 5. Typical morphology found in powder calcined at 1125 °C: (a) L/Ti sample, (b) G/Ti sample and (c) S/Ti sample.

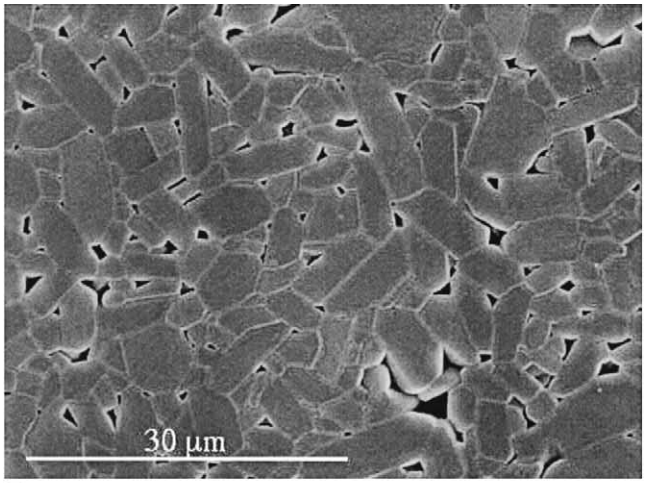

(a)

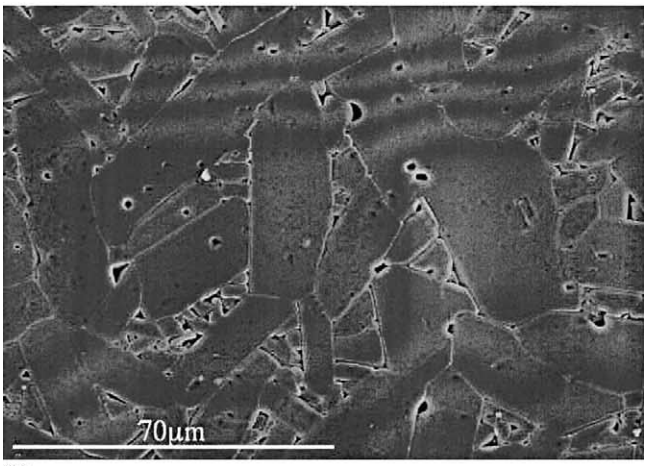

(b)

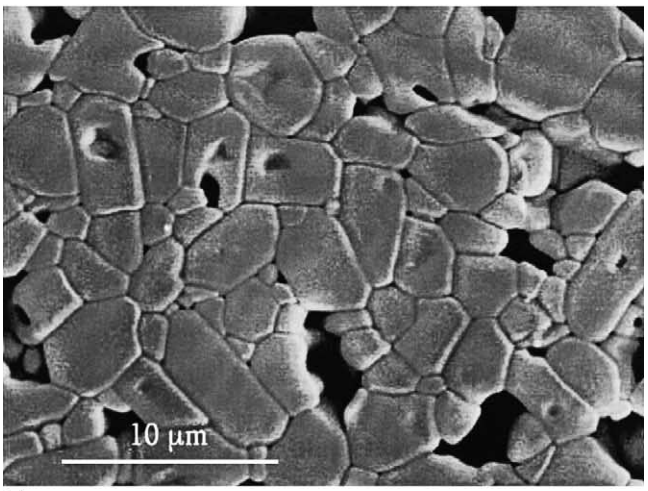

(c)

Fig. 6. Microstructure of titania-doped alumina sintered at 1625 °C for 4 h: (a) P/Ti sample, (b) C/Ti sample and (c) S/Ti sample.

5 nm) than the former ones. These particles show rounded shapes and a high degree of agglomeration. Some of these agglomerates have a sponge-like aspect, so, seems to indicate that this agglomeration is a soft type. However, other ones appear as a hard and compacted mass (in the same figure).

Powders obtained by the sol–gel process (S/Ti, Fig. 5c) also have corundum single crystals with hexagonal-like shapes, and vortices slightly rounded. This shows the vermicular shape of the α-alumina grains formed due to partial sintering between the grains. The particle size (below 100 nm) is in between the other two routes, Pechini and coprecipiation. Particles with sintered necks can also be observed, which make harder agglomerates to be processed under isopressing conditions.

The powder morphology as well as the particle agglomeration and the green density of each sample after isopressing deeply influences the sintering behaviour of the powders and the final density of the ceramics as it can be seen in the scanning electron micrographs shown in Fig. 6. In this case, the green density for the three specimens was similar, being higher for the C/Ti sample (46%) and lower for P/Ti and S/Ti specimens (about 40%).

The microstructures correspond to the sintered material at 1625 °C, being later mirror-like polished and thermally etched at 1550 °C. The micrography for P/Ti sample (Fig. 6a) reveals a homogenous microstructure in shape and size of elongated grains (about 7 μm × 3 μm) with a 92% of theoretical density. The high percentage of pores located at the triple points indicates an incomplete sintering process. Higher density (98%) was obtained in the C/Ti sample (Fig. 6b), that revealed a bimodal microstructure with two different kind of pores: intergrains characteristic of the sintering process and, intragrains due to the coalescence of grains. In fact, some grains exhibit exaggerated grain growth at the expense of the smallest ones giving planks of about 50 μm × 15 μm in size.

Finally, the S/Ti sample micrograph in Fig. 6c, shows mainly equiaxed grains of about 4 μm. A small percentage of grains present elongated shapes and sizes below 1 μm. This is the material with the lowest density, less than 90%, which is a consequence of the open porosity generated during sintering process.

4. Discussion

The α-alumina precursor obtained by each route of synthesis plays an important role in the morphological and microstructural characteristics of the titania-doped alumina material.

For the Pechini procedure and, taking into account that there is not any kind of precipitation process, it does not make sense to talk about aluminium hydrates as a forerunner of the aluminium oxide. In this case the hydroxycarboxylic acid (lactic acid) reacts with ethylene glycol to yield an ester compound, which can be confirmed by its infrared band at 1740 cm^{-1} characteristic of the carbonyl group and by the non-crystalline X-ray diffractogram.

Taking into account the relationship between the different phases in the Al_2O_3–H_2O system,[17] the synthesis method seems to determine greatly the precursor nature and the temperatures of dehydroxylation and conversion to other phases.

In spite of the greatest similarity between the coprecipitation and the sol–gel processes, where a precipitate phase was obtained, we have precluded the hypothesis of the development of the same precursor for both methods. On the other hand, the endothermic peak found in the thermal analysis for the C/Ti sample (Fig. 2b) was related to the gibbsite dehydroxylation. This phenomenon was not observed in the DTA for S/Ti sample where the endothermic peak found around 200 °C was assigned to the loss of absorbed water. Also, a difference can be distinguished through the infrared absorption spectra (Fig. 4) in the spectral range of the hydroxyl stretching (3650–2900 cm^{-1}). Hydroxyl stretching infrared absorption bands of synthetic boehmite and gibbsite have been published[18,19] to be at 3413, 3283, 3096 and 2977 cm^{-1} for boehmite and 3661, 3620, 3525, 3452, 3394, 3375 and 3338 cm^{-1} for gibbsite. These bands were well-resolved for synthetic samples, but in the present work the as-prepared samples at 25 °C showed overlapped bands due to the contribution of other species such as H–O–H, Al–O–H, Ti–O–H, C–O–H and C–H. However, it is possible to find some differences in the two spectra that allow to confirm that different precursors for C/Ti and S/Ti processes have been obtained.

Unlike the infrared spectra of the C/Ti sample with a narrow spectral range for the O–H stretching bands, the absorption bands characteristic of the boehmite were observed around 2900 cm^{-1} in the S/Ti spectrum. Gibbsite is the lower temperature aluminium hydrate and its hydroxylation takes places at low temperature. Obviously, the coprecipitation process takes place at room temperature where gibbsite is stable and its hydroxylation occurs at 260 °C, as it has been proved through DTA and the lack of spectral bands around 2900 cm^{-1}. Therefore, gibbsite-like precursors are predicted for the C/Ti process and the amorphous-like boehmite for the S/Ti process.

Dopants also determine the α-alumina precursors. Comparing titania-doped and undoped alumina obtained by the Pechini method, different intermediate phases in the crystallisation sequence were found.[14] Undoped alumina intermediate phases correspond to γ- and θ-alumina, while for the titania-doped material, the intermediate phase is κ-alumina.

The accommodation of the dopant in a specific structure varies with its nature. Some authors have reported that 1 mol% of doping element is enough to increase the phase transition to α-alumina up to 1315 °C,[20] which it has not been noticed in the present work using the Pechini synthesis and comparing with undoped alumina.[14] A study about the effect of the dopant concentration on the phase transition, keeping constant the synthesis route, will be described in a further paper.

Phase transformations are frequently accompanied by microstructural changes: particle agglomeration, diminution of the powder surface area as well as the growth of large-grained vermicular microstructures. This fact could explain the large microstructural differences between the three powders calcinated at 1125 °C. The structural transformations to well-crystallised α-alumina are described by nucleation and growth mechanisms. It is now interesting to comment that for the C/Ti sample the θ-alumina remains stable at this temperature. The measured activation energy of the $\theta \rightarrow \alpha$ transition is 650 kJ/mol, which is higher than 360 kJ/mol for the $\gamma \rightarrow \alpha$ transformation.[21] For the sample C/Ti, at 1125 °C, the grain growth is starting before transforming, and therefore, this explains the small size and rounded aspect of the particles (Fig. 5b).

For the sol–gel process, the α-alumina particles are clearly smaller than those obtained by the Pechini method. The particles and their morphology depend on the initial pH[22] of the reaction media. In this work, the acid hydrolysis by means of the addition of nitric acid leads to the formation of linear polymers and rounded particles. This favours the formation of sintering necks at the highest temperature used (1125 °C).

The large size and the hard aggregates formed in the calcining process in P/Ti and S/Ti, respectively, determine a non-optimum sintering behaviour. In this case the formed pores can be larger than the critical ratio to be eliminated which even would produce grain growth in the final sintering stage. The higher density obtained in C/Ti powder may be due to the in situ conversion of the low temperature θ-phase to α-alumina, as Sathiyakumar and Gnanam[23] pointed out.

Finally, it has been reported that the addition of small amounts of titania to alumina results in anisotropic grain morphology.[24] This effect is highly perceptible for C/Ti sample and medium for P/Ti. Nevertheless it was not detected for S/Ti probably due to the composition distribution is more homogeneous than in the other cases, so the segregation effects may be lower. The characteristic of the C/Ti material led to the severe anisotropic microstructure. The abnormal grain growth obtained is a result of different factors such as the initial microstructure and the dopants. The titania dopant may segregate in the grain boundary and can act in a variety of ways: changing the relative magnitude of the surface energies or the diffusional growth processes or simply avoiding the growth on specific surfaces.[25] This can lead to form elongated grains as those shown in the Fig. 6b.

5. Conclusions

The synthesis method of the titania-doped alumina materials determines the type of precursor of the intermediate phases as well as the temperature of dehydroxylation and conversion to other phases. Amorphous like boehmite and gibbsite-like precursors are predicted for the sol–gel and coprecipitation methods, respectively. These precursors trans-

form to κ-Al_2O_3, θ-Al_2O_3 and γ-Al_2O_3 for the Pechini, coprecipitation and sol–gel processes, respectively, as intermediate phases to develop α-Al_2O_3. None of other possible metastable phases were found.

The existence of dopants, as titanium, also determines the α-Al_2O_3 precursors. So, while γ- and θ-Al_2O_3 are the intermediate phases for undoped alumina in the Pechini process, κ-Al_2O_3 is the intermediate for the 1 wt.% titania-doped alumina.

Particles with the smallest size and rounded aspect were obtained via coprecipitation where θ-Al_2O_3 remains stable. In this case the activation energy required to the transformation to the alpha phase is larger than that require for the other methods like the sol–gel process where larger grains and vermicular shapes were found.

Pechini method leads to hexagonal morphology corresponding to corundum crystals of 1 μm in diameter.

Given that the morphology influences the sinter behaviour, different final densities of the material are obtained as a function of the method employed. The highest density (>98% *d*th) is obtained via coprecipitation where ultrafine particle size are obtained.

Acknowledgements

The authors are indebted to Mr. Alfonso Vidal and Miss Montserrat Martín for their help in these experiments. This work was supported by the MAT2001-1489-C02-01 CICYT project.

References

1. Xu, Q. and Anderson, M. A., Synthesis of porosity controlled membranes. *J. Mater. Res.* 1991, **6**, 1073–1080.
2. Anderson, M. A., Gieselmann, M. J. and Xu, Q., Titania and alumina ceramic membranes. *J. Membr. Sci* 1988, **39**, 243–258.
3. Walker, G. S., Williams, E. and Bhattacharya, A. K., Preparation and characterization of high surface area alumina–titania solid acids. *J. Mater. Sci.* 1997, **32**, 5583–5592.
4. Jansen, S. A., Grabatia, S. A. and Buecheler, N. M., Electronic properties of alumina/titania mixed oxides and interfacial surface models: a theoretical analysis. *Mater. Res. Soc. Symp. Proc*. 1993, **291**, 227–232.
5. Mehta, S. K. and Sengupta, S., Luminiscence and colour centres in Al_2O_3:Si,Ti. *Nucl. Instrum. Methods Phys. Res.* 1979, **164**, 349–354.
6. Taruta, S., Itou, Y., Takasugawa, N., Okada, K. and Otsuka, N., Influence of aluminium titanate formation on sintering of bimodal size-distributed alumina powder mixtures. *J. Am. Ceram. Soc*. 1997, **80**(3), 551–556.
7. Horn, D. S. and Messing, G. L., Anisotropic grain growth in TiO_2-doped alumina. *Mater. Sci. Eng. A* 1995, **195**, 169–178.
8. Fabris, S. and Elässer, C., First-principles analysis of cation segregation at grain boundaries in Al_2O_3. *Acta Mater.* 2003, **51**, 71–86.
9. Levin, I. and Brandon, D., Metastable alumina polymorphs: crystal structures and transition sequences. *J. Am. Ceram. Soc.* 1998, **8**, 1995–2012.
10. Segal, D., Chemical synthesis of ceramic materials. *J. Mater. Chem.* 1997, **7**(8), 1297–1305.
11. Pechini, M. P., US Patent, 3 330697, 1967.
12. Hernández, M. T., Osendi, M. and Jurado, J. R., Mullite and alumina/Y_2O_3–ZrO_2 composites as solid electrolytes. In *Third Euro-Ceramics, Vol 2*, ed. P. Durán and J. F. Fernández. Faenza Editrice, Iberica, Spain, 1993, p. 229.
13. Brinker, C. J. and Scherer, G. W., *Sol–Gel Science, the Physics and Chemistriy of Sol–Gel Processing*. Academic Press, New York, 1990, p. 263.
14. Hernández, M.T. and González, M., Synthesis of resins as alpha alumina precursors by the Pechini method using microwave and infrared heating. *J. Eur. Ceram. Soc*. 2002, **22**, 2861–2868.
15. Rama Rao, G. V., Venkadesan, S. and Saraswati, V., Susface area and pore size studies of alumina gels. *J. Non-Cryst. Solids.* 1989, **111**, 103–112.
16. Tarte, P., Infra-red spectra of inorganic aluminates and characteristics vibrational frequencies of AlO_4 tethaedra and AlO_6 octahedra. *Spectrochim. Acta* 1967, **23A**, 2127–2134.
17. Frost, R. L., Kloproge, J. T., Russell, S. C. and Szety, J. L., Dehydroxylation of aluminium(oxo)hydroxides using infrared emission spectroscopy. Part II: Boehmite. *Appl. Spectrosc*. 1999, **53**(5), 572–582.
18. Frost, R. L., Kloproge, J. T., Russell, S. C. and Szety, J. L., Vibrational spectroscopy and dehydroxylation of aluminium(oxo)hydroxides: Gibbsite. *Appl. Spectrosc*. 1999, **53**, 423–434.
19. Frost, R. L., Kloproge, J. T., Russell, S. C. and Szety, J. L., Vibrational spectroscopy of aluminium(oxo)hydroxides using infrared emission spectroscopy. Part III: Diaspore. *Appl. Spectrosc*. 1999, **53**, 829–835.
20. Rossignol, S. and Kappenstein, C., Effect of doping elements on the thermal stability of transition alumina. *Int. J. Inorg. Mater.* 2001, **3**, 51–58.
21. Mishra, P., Low-temperature synthesis of α-alumina from aluminium salt and urea. *Mater. Lett.* 2002, **55**, 425–429.
22. Sharma, P. K., Varadan, V. V. and K Varadan, V., A critical role of pH in the colloidal synthesis and phase transformation of nanosize-gamma-alumina with high surface area. *J. Eur. Ceram. Soc.* 2003, **23**, 659–666.
23. Sathiyakumar, M. and Gnanam, F. D., Synthesis of sol–gel derived alumina powder: effect of milling and calcination temperatures on sintering behaviour. *Br. Ceram. Trans.* 1999, **92**(2), 87–92.
24. Kebbede, A., Messing, G. L. and Carim, A. H., Grain boundaries in titania-doped α-alumina with anisotropic microstructure. *J. Am. Ceram. Soc.* 1997, **80**(11), 2814–2820.
25. Kwon, O.-S., Hong, S.-H., Lee, J.-H., Chung, U.-J., Kim, D.-Y. and Hwang, N. M., Microstructural evolution during sintering of TiO_2/SiO_2-doped alumina: mechanism of anisotropic abnormal grain growth. *Acta Mater.* 2002, **50**, 4865–4872.